

## Fluorescence line narrowing, localized exciton states, and spectral diffusion in the mixed semiconductor $\text{CdS}_x\text{Se}_{1-x}$

E. Cohen\* and M. D. Sturge

*Bell Laboratories, Murray Hill, New Jersey 07974*

(Received 4 November 1981)

We have observed fluorescence line narrowing in the LO-phonon-assisted intrinsic exciton emission of  $\text{CdS}_x\text{Se}_{1-x}$ , selectively excited over a range of energies below a critical energy  $E_{cm}$ , on the low-energy side of the exciton absorption line. The sharp emission lines disappear rather abruptly as the exciting energy increases through  $E_{cm}$  or as the temperature is raised above 10 K. We argue that this sharp line emission arises from excitons localized, on the time scale of the radiative lifetime (about 1 nsec), by alloy fluctuations. Its abrupt disappearance may be evidence for an effective mobility edge. A sideband on each of the sharp LO-phonon-assisted emission lines is also observed. The shape of this sideband can be accounted for by a model of spectral diffusion by acoustic-phonon-assisted tunneling between localized states.

### I. INTRODUCTION

Energy transfer between localized states is a subject of considerable current interest, both theoretically<sup>1,2</sup> and experimentally.<sup>3,4</sup> Most of the work has been done on open-shell impurities in insulating crystals and glasses,<sup>1,3</sup> or on mixed organic molecular crystals.<sup>4</sup> The less-studied case of exciton migration in semiconductors<sup>5</sup> is, however, of great interest, primarily because of the large diameter (up to 100 Å) of the exciton. This has two consequences: Exciton migration, if it occurs at all, must involve transport over relatively large distances, and the exciton-phonon interaction is confined to phonons of long wavelength. Excitons in mixed semiconductors show particular promise in this field since random fluctuations in the composition produce concomitant fluctuations in the band gap. The exciton states are thus inhomogeneously broadened by an amount which in many cases is larger than the energy of the long-wavelength acoustic phonons which can couple to the exciton, and which are involved in spectral diffusion. Contrary to the case of amorphous semiconductors, however, the fluctuations are not so large as to destroy the excitons completely, or even to localize them at the band center.

$\text{CdS}_x\text{Se}_{1-x}$  and  $\text{Cd}_x\text{Zn}_{1-x}\text{Te}$ , which are direct-gap semiconductors for all  $x$ , show a strong absorption line due to the formation of free excitons at  $\mathbf{k}=0$ . For  $x \neq 0$  or 1, this line has an inhomogeneous

width of about 10 meV<sup>6,7</sup> compared with perhaps 0.2 meV in a good crystal of CdS or CdSe. Similar results are obtained for  $\text{GaAs}_{1-x}\text{P}_x$  (Ref. 8) and  $\text{Ga}_{1-x}\text{Al}_x\text{As}$  (Ref. 9) for  $x < x_c$ , where  $x_c$  is the  $\Gamma$ -X crossover composition. Photoluminescence from exciton states is observed in all these mixed semiconductors when nominally pure; the emission peak obtained with nonresonant excitation is just below the free-exciton absorption peak and has a low-energy tail 10–50 meV wide. Some of the low-energy emission is associated with impurity-bound excitons, which are spectroscopically indistinguishable from intrinsic excitons bound by alloy fluctuations in this energy region.

In the following section we outline a model of exciton states in a random potential and show qualitatively how the Mott-Anderson picture<sup>10</sup> of localization below a mobility edge applies to it. We calculate the spectral diffusion due to one-phonon-assisted tunneling between localized states, considering both the piezoelectric and deformation-potential coupling mechanisms.

In Sec. III we describe our experimental procedure and results. We show that fluorescence line narrowing (i.e., the spectral sharpening of an emission line under selective excitation) occurs for excitons in  $\text{CdS}_x\text{Se}_{1-x}$ , with  $x=0.29, 0.53$ , and 0.9, below about 10 K. The narrowing is observed in the two LO-phonon sidebands of the exciton emission, which are sharp if the no-phonon line is sharp. Thus, the problem of detecting resonant

no-phonon fluorescence in the presence of scattered laser light is avoided. The narrowing occurs even for exciton energies where the absorption is so high ( $\sim 10^3 \text{ cm}^{-1}$ ) that the excitons must be intrinsic, not impurity bound. To our knowledge this is the first system in which such narrowing of an intrinsic exciton has been observed. We show that this observation probably implies that the excitons are localized on the timescale of the radiative lifetime ( $\sim 1 \text{ nsec}$ ).

We also report the observation of spectral diffusion which is strongly dependent on energy shift, and show that it can be accounted for quantitatively by the theory of Sec. II. Piezoelectric coupling is, as expected,<sup>11</sup> predominant, except at high  $x$  where there appears to be an anomalously large deformation potential contribution. A possible explanation of this anomaly is suggested.

A preliminary report of this work has already been given.<sup>12</sup> Independent work, over a small range of  $x$  on the same system, has been reported by Permogorov *et al.*<sup>13</sup> Their experimental results are essentially in agreement with ours; furthermore, they report induced polarization data which support our interpretation of the spectral diffusion.

## II. THEORY

### A. Exciton states in a mixed semiconductor

In  $\text{CdS}_x\text{Se}_{1-x}$  the exciton states are associated with the direct gap at the Brillouin-zone center.<sup>6</sup> In the virtual-crystal approximation, the internal energy-level structure is given by the effective-mass approximation, with electron and hole masses which can be interpolated between those of CdS and CdSe. The exciton binding energy is thus expected to vary from 29 to 16 meV and the exciton Bohr radius  $a_B$  from 25 to 45 Å.<sup>14,15</sup> We will be mainly concerned with the lowest 1S state, corresponding to the "A" ( $\sigma$  polarized) exciton. In mixed crystals, composition fluctuations  $\Delta x$  cause smearing of the band-edge absorption and fluorescence spectra. This phenomenon has been reported for many semiconductors. Its origin is thought to be fluctuations in the band gap due to the random fluctuations in composition, averaged over the volume occupied by the exciton.<sup>6,16</sup>

In this work we do not offer any direct evidence on the problem of the density of states in a random potential; rather, our interpretation assumes that this is a qualitatively correct description of

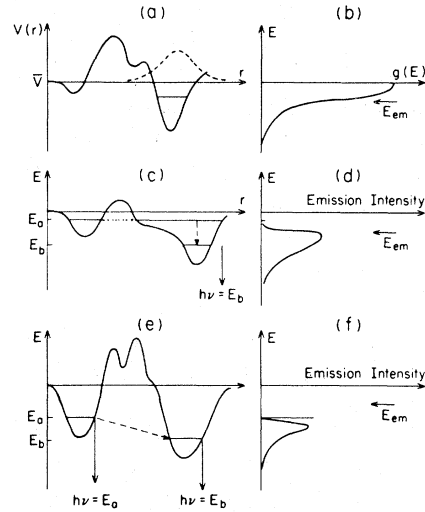


FIG. 1. (a) Schematic representation of  $V(\vec{r})$ .  $E$  is the energy of an exciton state bound by a potential fluctuation; the corresponding wave function is indicated by the dashed line. (b) The density of states  $g(\epsilon)$  (schematic) in the potential  $V(\vec{r})$ .  $E_{em}$  is the effective mobility edge (see text). (c) Resonant transfer at energy  $E_a$ , followed by phonon emission to a localized state of energy  $E_b$  and subsequent radiation. (d) The expected emission spectrum for excitation above the mobility edge. (e) Nonresonant transfer between localized states involving phonon-assisted tunneling. (f) The expected emission spectrum for excitation below the mobility edge.

the exciton states with which we are dealing. For specificity, we outline a density-of-states model based on the calculations of Halperin and Lax,<sup>17</sup> and show that it leads naturally to the Mott-Anderson concept of an energy called the "mobility edge," which separates localized from delocalized exciton states. The potential felt by an exciton at the point  $\vec{r}$  is written as

$$V(\vec{r}) = \bar{V} + v(\vec{r}), \quad (1)$$

where  $\bar{V}$  is the average potential (i.e., the  $k=0$  exciton energy in the virtual-crystal approximation) and

$$v(\vec{r}) = \left\langle \frac{dV}{dx} \right\rangle \Delta x(\vec{r}). \quad (2)$$

$\Delta x(\vec{r})$  is the composition fluctuation averaged over a volume  $R^3$  ( $R \geq a_B$  where  $a_B$  is the exciton Bohr radius), centered on  $\vec{r}$ . This potential is schematically represented in Fig. 1(a). An exciton will be bound in the potential well caused by the fluctua-

tions if  $|v| \gtrsim \hbar^2/m_x R^2$ , where  $m_x$  is the exciton mass. In Ref. 17 the Schrödinger equation for a particle in such a well is solved, subject to the condition that the fluctuation is the most probable one satisfying the above condition for binding. The calculations yield a density of states  $g(\epsilon)$  which in the low-energy tail has the form

$$g(\epsilon) = g_0(\epsilon) \exp \left[ - \left[ \frac{\epsilon}{\epsilon_0} \right]^{a(\epsilon)} \right], \quad (3)$$

with  $a \sim 1$  and  $g_0^{-1} \sim \epsilon_0 a_B^3$  in range of interest. A similar result is obtained by Lai and Klein,<sup>18</sup> based on the calculations of Sayakanit.<sup>19</sup> This is illustrated in Fig. 1(b). Here  $\epsilon = \bar{V} - E$  is the energy measured downwards from the bottom of the exciton band of the virtual crystal (i.e., that obtained by neglecting potential fluctuations) which we take to be the position of the observed absorption peak;  $\epsilon_0 \sim m_x a_B^2 \langle v^2 \rangle / 4\hbar^2$ . This expression for  $\epsilon_0$  is obtained<sup>17</sup> if we take  $a_B/2$  to be a measure of the correlation length of  $v(r)$ , as seen by the exciton (i.e.,  $Q^{-1}$  in the notation of Ref. 17). That is, we assume that

$$\langle v(\vec{r})v(0) \rangle \sim \langle v^2 \rangle e^{-2r/a_B}. \quad (4)$$

Following Goede *et al.*,<sup>6</sup> we take

$$\langle v^2 \rangle \sim \left[ \frac{dE_g}{dx} \right]^2 x(1-x)\Omega/\pi a_B^3, \quad (5)$$

where  $\Omega$  is the atomic volume and  $E_g$  the band gap. Substituting the numbers for  $x \sim \frac{1}{2}$  we find  $\epsilon_0 \sim 3$  meV.

The average separation  $\langle R \rangle$  of the states in a range  $\Delta E$  about  $\epsilon$  is

$$\langle R \rangle \sim [g(E)\Delta E]^{-1/3}.$$

Resonant transfer from one site to another will be possible if the transfer matrix element  $M$  satisfies  $M \gtrsim \Delta E$ . For tunneling between isolated states,

$$M \sim \epsilon \exp[-(2m_x \epsilon)^{1/2} \langle R \rangle / \hbar]. \quad (6)$$

Transfer will be possible and the state delocalized if a value of  $\Delta E$  can be found which satisfies

$$\ln(\epsilon/\Delta E) \gtrsim \hbar^{-1}(2m_x \epsilon)^{1/2} [g(\epsilon)\Delta E]^{-1/3}.$$

For sufficiently small  $g(\epsilon)$ , no such  $\Delta E$  can be found. Thus transfer is not possible for  $\epsilon \gtrsim \beta \epsilon_0$ , where  $\beta$  is a numerical factor of order 1 which depends on the details of the model. Thus, we expect a Mott-Anderson "mobility edge" at  $\epsilon = \beta \epsilon_0$ , with localized states, amongst which transfer can

only occur by thermally activated hopping below it and propagating bandlike states above it. (This is, of course, a greatly simplified version of a very sophisticated theory.)

The existence of a mobility edge in a disordered system has never been satisfactorily established experimentally. This may be because of the complications introduced by "off-diagonal" disorder (i.e., fluctuations in the transfer matrix elements rather than in the potential<sup>20</sup>) and by Coulomb interaction between charged particles.<sup>21</sup> In the present case we are dealing with neutral particles (excitons) whose interactions can be neglected at low densities, and the latter difficulty does not apply.

The Mott-Anderson picture of a well-defined mobility edge assumes that the line broadening is "microscopic," i.e., that there is no correlation between band gap and position in space. This means that at any particular site where the energy is  $E_a$ , the probability  $p(E_b)$  of another site of energy  $E_b$  being at position  $\vec{R}$  depends only on the density of states  $g(E_b)$ . Only in this case is Mott's argument<sup>10</sup> that localized and delocalized states cannot coexist at the same energy valid. In a real solid "macroscopic" broadening also occurs. In this case  $p$  is a function of  $E_a$  and  $R$ , as well as of  $E_b$ , due to long-range variations in potential over and above the random-alloy fluctuation. Such long-range variation could arise from fluctuations in growth conditions or from strain. In this case, states of the same energy may be localized in one part of the crystal and delocalized in another, being unable to communicate with each other. Thus, the mobility edge can be broadened. We will see that macroscopic broadening may play an important role in the tail of the exciton band under study here.

Further complications must be considered before experimental data can be interpreted. There is the question of timescale. The Mott-Anderson picture assumes infinite time (i.e., it considers the dc conductivity). In fact, excitons in a direct-gap semiconductor such as  $\text{CdS}_x\text{Se}_{1-x}$  only live for about 1 nsec. Thus, in a selective excitation experiment, where excitons are created with a particular energy and their spectral diffusion observed, there can be an "effective" mobility edge  $E_{em}$ , only above which is exciton motion possible with the decay time. Even in the absence of macroscopic broadening, there is no reason to expect this "edge" to be sharp.

An exciton created at a point where its energy

$E_a$  is greater than  $E_{em}$  is in a band (delocalized) state and has a finite probability of being in the vicinity of a localized state with energy  $E_b < E_{em}$  [see Fig. 1(c)]. Here it will quickly thermalize to  $E_b$  by phonon emission, and a photon of energy  $E_b$  will be emitted. Thus, excitation above  $E_{em}$  will produce emission only at energies below  $E_{em}$  [Fig. 1(d)]; i.e., spectral diffusion is rapid. An exciton created below  $E_{em}$ , on the other hand, will decay resonantly on the same site. Thus fluorescent line narrowing can occur, observable in the present case of  $\text{CdS}_x\text{Se}_{1-x}$  through sharp LO-sideband emission.

So far we have ignored the possibility of phonon-assisted tunneling [Fig. 1(e)]. Because this is a nonresonant process, it permits spectral diffusion below the mobility edge (effective or real). If the rate of tunneling is less than or comparable with the radiative decay rate, a sharp resonant emission at  $E_a$  (the exciting energy) will be observed, accompanied by a sideband and whose spectral shape reflects the energy dependence of the tunneling probability [Fig. 1(f)]. This process is discussed in the following sections.

If the rate of phonon-assisted tunneling is much faster than the radiative rate, no resonant emission will be seen and the cw spectrum will be indistinguishable from that expected for excitation into the delocalized states above  $E_{em}$ .

The model we have described here, while plausible, has not been directly verified experimentally in any semiconductor. There is some spectroscopic evidence that excitons localized by alloy fluctuations exist in the extreme tail of the indirect exciton in  $\text{GaAs}_x\text{P}_{1-x}$ .<sup>18</sup> In the present study we will present evidence that the states in the low-energy tail of the direct exciton of  $\text{CdS}_x\text{Se}_{1-x}$  are indeed localized on a time scale of order 1 nsec, and that spectral diffusion occurs by phonon-assisted tunneling between these localized states.

Exciton states near the absorption maximum are generally thought to be describable in the virtual-crystal approximation, which means that they are delocalized. However, there is little evidence for this, at least in the present case of  $\text{CdS}_x\text{Se}_{1-x}$ . If it is true, there must be a changeover from localized to delocalized states somewhere in the band; i.e., a (not necessarily sharp) mobility edge.

## B. Exciton-phonon interaction

In the process of nonresonant transfer between sites corresponding to different exciton energies, the energy mismatch is taken up by acoustic phonons. The exciton-phonon interaction Hamiltonian, in the case where phonons can be described by a wave vector  $\vec{q}$ , has the form<sup>22</sup>

$$H_{xp} = [F_e(s, q)e^{i\vec{q} \cdot \vec{r}_e} + F_h(s, q)e^{i\vec{q} \cdot \vec{r}_h}] \times [b_s^\dagger(-q) + b_s(q)]. \quad (7)$$

Here  $b_s^\dagger(q)$  and  $b_s(q)$  are the phonon creation and annihilation operators (branch  $s$ ),  $\vec{r}_e$  and  $\vec{r}_h$  are the electron and hole coordinates, respectively, and  $F_e(s, q)$  [ $F_h(s, q)$ ] are the electron (hole) -phonon interaction matrix elements which depend on the mechanism of interaction. Two types of interactions have been considered for acoustic phonons. The first is the deformation potential for which<sup>1</sup>

$$F_{e,h}^D(s, q) = (\hbar q / 2\rho v_s)^{1/2} E_{c,v}. \quad (8)$$

$E_{c,v}$  is the relevant deformation potential of the conduction (valence) band,  $\rho$  is the crystal density, and  $v_s$  is the sound velocity for the  $s$ -phonon branch. The dominant contribution is from longitudinal (LA) phonons. The second type is the piezoelectric interaction, which has the following matrix element in crystals with the wurtzite structure<sup>11,23,24</sup>:

$$F_e^P(s, q) = \frac{4\pi e}{\kappa} \left[ \frac{\hbar}{2\rho v_s q} \right]^{1/2} \{ e_{15} \sin\theta [U_z(s, q) \sin\theta + U_y(s, q) \cos\theta] + e_{13} U_y(s, q) \sin\theta \cos\theta + e_{33} U_z(s, q) \cos^2\theta \}. \quad (9)$$

Here,  $\kappa$  is the dielectric constant,  $U(s, \vec{q})$  is the displacement vector of the atoms in the unit cell,  $z$  is parallel to the  $c$  axis and  $y$  lies in the  $q$ - $z$  plane, and  $\theta$  is the angle between  $\vec{q}$  and the  $z$  axis. The  $e_{ij}$  given are the only nonzero components of the piezoelectric tensor. The angular factors in Eq. (9)

can be spherically averaged to give effective piezoelectric constants for LA and TA phonons, respectively,<sup>25</sup>

$$\langle e_{LA}^2 \rangle_\theta = \frac{1}{7} e_{33}^2 + \frac{4}{35} e_{33} (e_{31} + 2e_{15}) + \frac{8}{105} (e_{31} + 2e_{15})^2, \quad (10a)$$

$$\langle e_{TA}^2 \rangle_{\theta} = \frac{2}{35} (e_{33} - e_{31} - e_{15})^2 + \frac{16}{105} e_{15} (e_{33} - e_{31} - e_{15}) + \frac{16}{35} e_{15}^2. \quad (10b)$$

These are roughly equal in CdS (see Table I). However, the greater density of states for TA phonons makes their contribution predominant, and piezoelectric coupling to LA phonons can usually be neglected.

### C. Energy transfer between localized exciton states

In this section we consider the basic transfer mechanism between localized excitons. We assume that an exciton is localized at a site  $\vec{R}_a$  with binding energy  $E_a$ . At temperatures such that  $kT \ll E_a$ , excitons can only move to a site  $R_b$ , with binding energy  $E_b$ , by a phonon-assisted tunneling process in which the phonon (or phonons) takes up the excess energy  $E_{ab} = E_a - E_b$ . This process is similar to that considered for paramagnetic ions in insulators<sup>1</sup> and we shall adapt this theory to the present case. The transfer matrix element for a single-phonon process is given by [Eq. (12) of Ref. 1]:

$$t^{(1)} = \frac{J(R) e^{i\vec{q} \cdot \vec{R}_a}}{\Delta E_{ab}} (M_{xp}^b e^{i\vec{q} \cdot \vec{R}} - M_{xp}^a), \quad (11)$$

where

$$M_{xp}^a = \langle X(\vec{R}_a), n_s(\vec{q}) \pm 1 | H_{xp} | X(\vec{R}_a), n_s(q) \rangle.$$

$|X(\vec{R}_a)\rangle$  is the wave function of the exciton localized at  $\vec{R}_a$ ,  $\vec{R} = \vec{R}_a - \vec{R}_b$ ,  $n_s(\vec{q})$  is the phonon occupation number, and

$$J(R) = \langle X(R_a) | H_{ss} | X(R_b) \rangle,$$

where  $H_{ss}$  is the intersite transfer Hamiltonian which may be exchange [ $J \sim \exp(-R/a_B)$ ], dipole-dipole ( $J \sim R^{-3}$ ), etc. Note that for excitons the electron and hole correspond to the excited and ground states, respectively, in the formalism of Ref. 1. The orientation-averaged transition rate for single-phonon-assisted transfer is<sup>1</sup>

$$W_{ab} = \frac{2\pi}{\hbar} \frac{J^2(R)}{\Delta E_{ab}} \sum_{s, \vec{q}} [ |M_{xp}^a|^2 + |M_{xp}^b|^2 - 2h(qR) \times |M_{xp}^a M_{xp}^b| ] \delta(\hbar\omega(q) - \Delta E_{ab}), \quad (12)$$

where

$$h(qR) = \sin qR / qR.$$

$(1-h)$  is the "coherence factor" of Ref. 1, the importance of which depends on the range of  $J(R)$ . If  $J \sim e^{-R/a_B}$ , the average value of  $h$  is

$$\langle h(qR) \rangle = \frac{\langle J^2(R) h(qR) \rangle}{\langle J^2(R) \rangle} = (1 + qa_B)^{-2}.$$

TABLE I. Parameters for exciton-phonon coupling in CdS<sub>x</sub>Se<sub>1-x</sub>.

	CdS	CdSe	CdS <sub>0.53</sub> Se <sub>0.47</sub>
$m_e/M_0$	0.205 <sup>a</sup>	0.13 <sup>b</sup>	0.17
$m_h/M_0$	0.98 <sup>a</sup>	0.63 <sup>b</sup>	0.82
$E_c$ (eV)	3.9 <sup>c</sup>	4.3 <sup>c</sup>	4.1
$E_v$ (eV)	1.3 <sup>c</sup>	1.5 <sup>c</sup>	1.4
$\langle e_{LA}^2 \rangle$ (Cm <sup>-2</sup> )	0.034 <sup>d</sup>	0.014 <sup>e</sup>	0.025
$\langle e_{LA}^2 \rangle$ (Cm <sup>-2</sup> )	0.041 <sup>d</sup>	0.019 <sup>e</sup>	0.031
$\kappa$	8.7 <sup>a</sup>	8.4 <sup>b</sup>	8.6
$a_B$ (Å)	28 <sup>a</sup>	42 <sup>b</sup>	35
$v_1$ ( $\times 10^5$ cm/sec)	4.25 <sup>f</sup>	3.7 <sup>e</sup>	3.95
$v_t$ ( $\times 10^5$ cm/sec)	1.76 <sup>f</sup>	1.54 <sup>e</sup>	1.66

<sup>a</sup>Reference 14.

<sup>b</sup>Reference 15.

<sup>c</sup>P. L. Camphausen, C. A. N. Connell, and W. Paul, Phys. Rev. Lett. **26**, 184 (1971); D. W. Langer, K. N. Euwema, K. Era, and T. Koda, Phys. Rev. B **2**, 4005 (1970).

<sup>d</sup>Reference 25.

<sup>e</sup>P. Y. Yu, Solid State Commun. **19**, 1087 (1976).

<sup>f</sup>Reference 11.

Since, experimentally, we only have data for  $qa_B \gtrsim 1$ , the term in  $h$  can be neglected. If we assume, as is reasonable for an allowed transition in a direct-gap semiconductor, that the variation of  $M_{xp}$  from site to site can be neglected, we obtain

$$W_{ab}(R) = \frac{4\pi}{\hbar} \frac{J^2(R)}{\Delta E_{ab}} \sum_{s,q} |M_{xp}|^2 \delta(\hbar\omega(q) - E_{ab}). \quad (13)$$

Note that for  $qa_B \rightarrow 0$ ,  $h \rightarrow 1$ , and we would have

$$W_{ab} \propto |M_{xp}^a - M_{xp}^b|^2 + (qa_B)^2 |M_{xp}|^2,$$

as discussed in Ref. 1. In this case the variation from point to point of  $M_{xp}$  obviously cannot be neglected.

Turning now to the evaluation of  $|M_{xp}|^2$ , we can factor out the dependence on the electron and hole coordinates to obtain, for a hydrogenic 1S exciton<sup>11,26</sup>:

$$\langle 1S | e^{i\vec{q} \cdot \vec{r}} \epsilon_{e,h} | S \rangle = \left[ 1 + \left( \frac{m_{h,e} qa_B}{2(m_e + m_h)} \right)^2 \right]^{-2} \equiv \alpha_{e,h}. \quad (14)$$

Summing over final states we obtain, for phonon emission (absorption),

$$W_{ab} = \frac{4\pi}{\hbar} J^2(R) G^2(\alpha, q) \frac{f(\Delta E_{ab})}{\Delta E_{ab}^2} \times g(E_b) \begin{cases} n_s(q) + 1 \\ n_s(q), \end{cases} \quad (15)$$

where  $f(E)$  is the density of phonon states,  $g(E)$  the density of (final) exciton states, and  $G^2(\alpha, q)$  depends on the mechanism of interaction. For deformation-potential coupling,

$$G_D^2 = \frac{\hbar q}{2\rho v_e} (E_c \alpha_e - E_v \alpha_h)^2. \quad (16)$$

While for piezoelectric coupling,

$$G_p^2 = \left[ \frac{e}{\kappa} \right]^2 \frac{\hbar}{2\rho v_l q} (\alpha_e - \alpha_h)^2 \langle e_{TA}^2 \rangle. \quad (17)$$

Here  $v_l$  and  $v_t$  are the longitudinal and transverse sound velocities averaged over angle.

Since the density of phonon states  $f(\Delta E_{ab})$  is proportional to  $\Delta E_{ab}^2$ , the entire dependence of  $W_{ab}$  on  $\Delta E_{ab}$  ( $= q\hbar v_s$ ) comes from the dependence of  $G^2$  and from  $g(E_b)$ . The  $q$  dependence of  $G_D^2$  and  $G_p^2$  is shown in Fig. 2. The coupling parameters for  $\text{CdS}_{0.53}\text{Se}_{0.47}$ , linearly interpolated from those for CdS and CdSe, are given in Table I. Note that

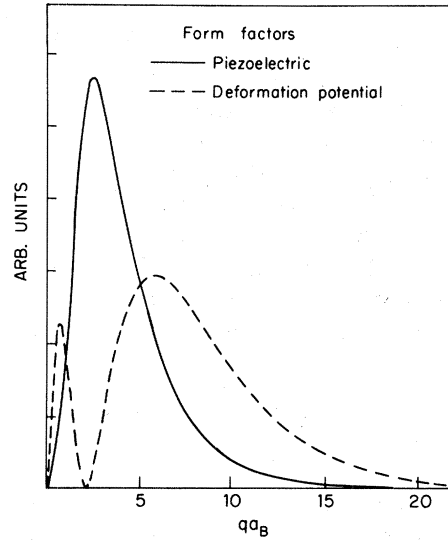


FIG. 2. Calculated relative probabilities for one-phonon-assisted tunneling as functions of  $qa_B$ , where  $q$  is the phonon wave vector and  $a_B$  the exciton Bohr radius. These curves are normalized to unit area and do not include the effect of the density of final exciton states. Full line represents piezoelectric coupling  $G_p^2$ ; dashed line represents deformation-potential coupling  $G_D^2$  for the particular choice of  $E_v$  and  $E_c$  given in Table I. Note that only  $E_c - E_v$  is determined experimentally; for the separate values we depend on theory, and the precise shape of the sideband is very sensitive to the assumed  $E_c/E_v$  ratio.

these numbers apply to free excitons and that they imply  $G_D^2 \ll G_p^2$ , except at very small  $q$ .

Since we appear to be dealing with localized excitons, the phonon interaction may not be the same as for free excitons. Piezoelectric coupling is a long-range interaction and is unlikely to be affected by details of the binding potential. For deformation-potential coupling, on the other hand, there can, in principle, be a strong effect since the binding energy of an exciton to an alloy fluctuation is likely to be strongly dependent on the precise atomic configuration in the region where the binding potential is strong. Such enhanced sensitivity to deformation has been observed, for example, in the exciton bound to nitrogen in GaP,<sup>27</sup> and for the "M" exciton in  $\text{GaAs}_{1-x}\text{P}_x$ ,<sup>28</sup> which is thought to be bound to alloy fluctuations.<sup>18</sup> This should lead to enhanced coupling to LA phonons with  $qa_B \sim 1$ , since  $a_B$  is a measure of the range of the potential well which binds the exciton. We shall see that for  $\text{CdS}_x\text{Se}_{1-x}$  with  $x \sim 0.9$ , where  $a_B$  is relatively small, such  $q$ -dependent enhancement of the deformation-potential coupling may be ob-

served.

The theory can readily be extended to two-phonon processes. "Raman" processes, in which one phonon is absorbed and one emitted, are of great importance in insulators such as ruby,<sup>29</sup> since they involve phonons of large  $q$ , and hence are not restricted by the coherence factor  $h(qR)$  discussed above. They may well be responsible for the disappearance of the sharp line above 10 K which we observe (see Sec. III). They should not be important at lower temperatures where  $kT \ll E_{ab}$ .

#### D. Spectral diffusion between localized exciton states

In Sec. II C we have shown that the exciton transfer rate between two sites depends both on the site separation [through  $J(R_{ab})$ ] and on the difference in binding energy ( $E_{ab}$ ). Our task now is to establish a model which will describe multiple-exciton transfer between localized sites within the radiative lifetime. This problem has been treated by Huber and Ching,<sup>2,30</sup> who calculated the luminescence spectrum at various time intervals after a monochromatic pulse excitation. They assumed an explicit form for both  $J(R_{ab})$  and  $g(E)$ . We shall adopt their approach, but as we do not have the precise form of  $J$  and  $g$  we shall have to make some simplifying assumptions.

Let  $P_a(t)$  denote the probability that an exciton occupies a site with binding energy  $E_a$  at time  $t$ . Excitons are created with monochromatic light and subsequently migrate between sites, losing energy by emitting phonons (at low temperatures). We assume that there is no correlation between  $E_{ab}$  and  $R_{ab}$ , so that Eq. (12) can be integrated over  $R$ . Taking  $J = J_0 \exp(-R/a_B)$ , we find for low temperature

$$w_{ab}(\Delta E_{ab}) = \frac{32\pi^2}{\hbar} J_0^2 a_B^3 G^2(\alpha, q) \frac{f(\Delta E_{ab})}{\Delta E_{ab}^2} g(E_b), \quad (18)$$

which can be simplified to

$$w(\Delta E_{ab}) = \delta(E_a) G'^2(E_{ab}) g'(E_b), \quad (19)$$

where

$$G'^2 = G^2 / \int G^2(E_{ab}) dE_{ab}$$

and

$$g'(E_b) = g(E_b) / g(E_a).$$

The parameter  $\delta(E_a)$  represents the overall nonradiative transfer rate at this energy and is treated as

an adjustable parameter. The problem is thus converted from exciton migration to that of spectral transfer, which is what is actually observed in our experiments. The set of rate equations appropriate to this problem is

$$\frac{dP_a(t)}{dt} = -\frac{P_a(t)}{\tau} - \sum_b w_{ab} P_a(t) + \sum_b w_{ba} P_b(t), \quad (20)$$

where  $\tau$  is the radiative lifetime. Since our measurements are all under cw or quasi-cw (pulse length  $\gg \tau$ ) conditions, the term in  $dP/dt$  can be neglected. At low temperatures ( $kT \ll \Delta E_{ab}$ ) we have no back transfer of excitation. Then if  $\tau\delta$  is sufficiently small, only a single phonon-assisted transfer can occur within a radiative lifetime, and we have for the intensity ratio

$$\frac{P_b}{P_a} = \frac{w_{ab}(\Delta E_{ab})}{\tau^{-1} + \sum w_{ab}} = \delta' G'^2(\Delta E_{ab}) g'(E_b), \quad (21)$$

where

$$\delta' = \frac{\tau\delta}{1 + \tau\delta}.$$

For multiple transfers we simply convolute this with itself, giving

$$\frac{P_b}{P_a} = \sum_n \delta'^n [G'^2 g]^n, \quad (22)$$

where  $[A]^n$  represents the result of convoluting  $A$  with itself  $n$  times.

The reader may be puzzled by the difference between Eq. (22) and the well-known equation for a radiative multiphonon sideband, which is of the form<sup>31</sup>

$$I(\omega) \sim e^{-S} \sum_n \frac{1}{n!} S^n [A(\omega)]^n, \quad (23)$$

where  $A(\omega)$  is the spectrum of coupling to phonons and  $S$  the coupling parameter analogous to  $\delta$ . The difference is a consequence of different statistics: in the multiphonon case the phonons are indistinguishable, whereas in the present case there is a real, distinguishable, intermediate electronic state between each phonon-assisted process.

An example of the results obtained is shown in Fig. 3. The most important result is that in the tail, where  $\tau\delta \ll 1$ , the line shape is independent of the excitation energy. Although the results shown in Fig. 3 (for excitation deep in the tail) were obtained for the particular choice of  $g(E_b)$  as an ex-

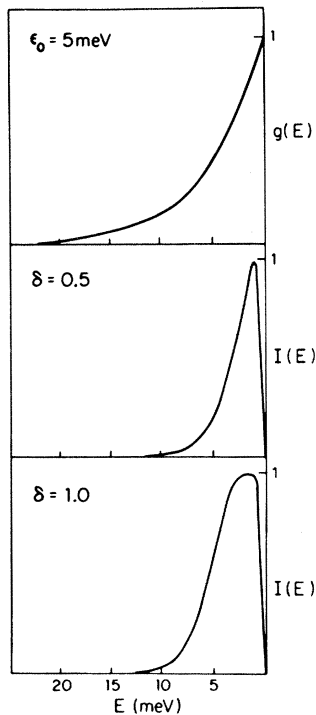


FIG. 3. Calculated spectra for phonon-assisted tunneling assuming piezoelectric coupling only. Parameters used are given in Table I for  $x=0.53$ . An exponential density of states  $g(E)$  is assumed and the parameter  $\delta$  is defined in Eq. (19).

ponential, similar results were obtained with a Gaussian. This means that the most important factor which determines exciton spectral diffusion is  $G^2(E_{ab})$ , namely, the energy dependence of the exciton-phonon interaction.

### III. EXPERIMENTAL

#### A. Experimental procedure

Single-crystal platelets of  $\text{CdS}_x\text{Se}_{1-x}$ , 100–200  $\mu\text{m}$  thick, were used in this study. They were grown by vapor transport with no intentional doping. The impurity content was not determined by any electrical measurements. However, the crystals show much weaker donor-acceptor emission bands than those reported in the literature for “undoped”  $\text{CdS}$ ,<sup>32</sup> which implies that the donor and acceptor concentration is less than  $10^{16} \text{ cm}^{-3}$ . Samples were mounted in a variable-temperature dewar (immersed in either liquid He or a flow of cold He gas). Temperature was varied between 2–20 K.

Photoluminescence spectra were obtained by selective excitation using either a cw dye laser pumped by an  $\text{Ar}^+$  ion laser or a pulsed dye laser pumped by a  $\text{N}_2$  laser. The cw dye laser has a linewidth of  $0.3 \text{ \AA}$  and its power density at the sample surface was  $0.2 \pm 0.1 \text{ W/cm}^2$ . (This uncertainty arises from the transfer characteristics of the optical components.) The pulsed dye-laser linewidth was  $0.6 \text{ \AA}$ , its pulse width was 1.5 nsec in the red and 1 nsec in the green. The power density at the sample surface ranged from  $10^{-4}$ – $10^{-6} \text{ J/cm}^2$  per pulse. The fluorescence was monitored with a double monochromator (resolution of  $0.5 \text{ \AA}$ ). Absorption spectra were taken with a Cary 14 spectrometer, and corrected for the dispersion in the refractive index.<sup>33,34</sup>

### IV. RESULTS

Crystals with  $x=0.29$ , 0.53, and 0.9 were studied: The most thorough examination was of a 100- $\mu\text{m}$ -thick platelet with  $x=0.53$ . The reflectance spectrum at 2 K shows peaks at 2.124 eV ( $\vec{E} \perp c$ ) and 2.145 eV ( $\vec{E} \parallel c$ ), corresponding to the “A” and “B” excitons, respectively. Figure 4 shows the absorption spectrum of this sample for  $\vec{E} \perp c$ . Absorption for  $\vec{E} \parallel c$  is too weak to measure in this region. The absorption coefficient  $\alpha(h\nu)$  in this region can be fitted to

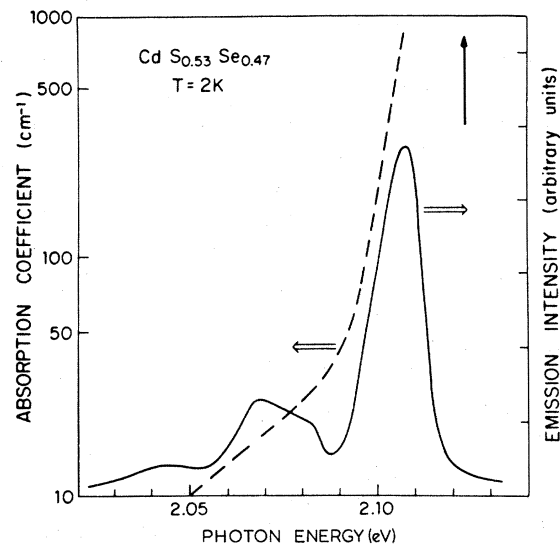


FIG. 4. Absorption (dashed line) and fluorescence (full line) spectra of  $\text{CdS}_{0.53}\text{Se}_{0.47}$  at 2 K. The fluorescence is obtained with excitation at 2.54 eV, well above the band gap.



$$\alpha(h\nu) = \alpha_1 e^{(h\nu - E_x)/E_1} + \alpha_2 e^{(h\nu - E_x)/E_2}, \quad (24)$$

with  $E_x = 2.124$  eV,  $\alpha_1 = 10^4$  cm<sup>-1</sup>,  $E_1 = 5$  meV,  $\alpha_2 = 100$  cm<sup>-1</sup>, and  $E_2 = 30$  meV. In the region where the slope is  $E_1$  the absorption is so strong that it must be intrinsic; hence we can put  $\epsilon_0 = E_1 = 5$  meV in agreement with the estimate of 3 meV in Sec. II A. However, as we shall see, there is probably a contribution to  $E_1$  from macroscopic broadening: this is thus an upper limit to  $\epsilon_0$ . In the region with slope  $E_2$  the absorption is probably due to impurities. All the emission data to which we refer subsequently were obtained with excitation in the  $E_1$  (intrinsic) region. Also shown is the fluorescence spectrum at  $T = 2$  K, excited with the 4880-Å line of an Ar<sup>+</sup>-ion laser. Comparison with the absorption spectrum shows that the emission band is due to tail states extending some 30 meV below the peak of the exciton line. The bands centered at 2.075 and 2.04 eV are the one-phonon and two-phonon sidebands of the non-phonon band centered at 2.108 eV. This can be seen clearly in the selectively excited luminescence spectra shown in Fig. 5, for which  $\vec{E} \perp c$  in both absorption and emission [ $(xy)x$  geometry in the conventional notation of Raman scattering]. In Fig. 5(a) the exciting laser energy  $E_{exc} = 2.092$  eV corresponds to the low-energy end of the intrinsic region of the exciton line. The spectrum consists of two sharp lines, 0.7 meV wide, with "sidebands" on the low-energy side, about 4 meV wide. The sharp lines, which are only observed in the  $\vec{E} \perp c$  spectrum, have energies 25.5 and 37 meV below the laser line; these correspond to the known LO<sub>1</sub> and LO<sub>2</sub> phonons.<sup>35</sup> Additional weaker bands separated by  $52 \pm 1$ ,  $63 \pm 1$ , and  $74 \pm 1$  meV correspond to 2LO<sub>1</sub>, LO<sub>1</sub> + LO<sub>2</sub>, and 2LO<sub>2</sub> phonons. Much weaker three-LO phonon lines can also be observed (not shown in the figure). Spectra identical to that shown in Fig. 5(a) are obtained with excitation energies in the range 2.085–2.105 eV. For  $E_{exc}$  below 2.085 eV, a broad (50-meV wide) donor-acceptor recombination band dominates the spectrum, although the sharper LO<sub>1</sub> and LO<sub>2</sub> features can still be discerned. For  $E_{exc}$  greater than 2.105 eV the sidebands broaden at the low-energy end. Typical spectra are shown in Figs. 5(b)–5(d). The broadening increases gradually with increasing  $E_{exc}$  but the two sharp lines still appear at the LO<sub>1</sub> and LO<sub>2</sub> phonon energies. These lines disappear abruptly for  $E_{exc}$  above 2.116 eV [Fig. 5(d)].

The sharp lines might naturally be thought to be

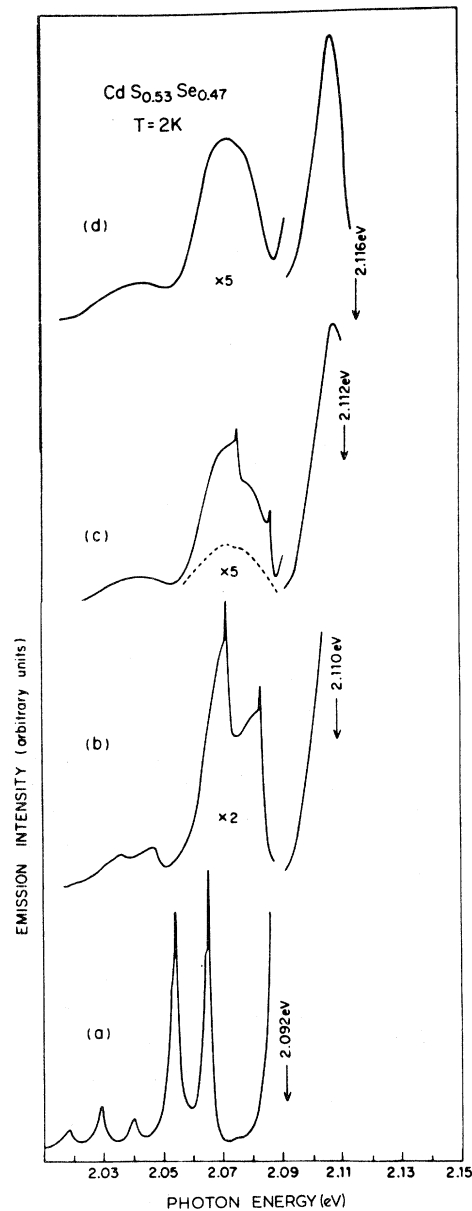


FIG. 5. Emission spectra under selective excitation of CdS<sub>0.53</sub>Se<sub>0.47</sub> at 2 K. The exciting laser is tuned to the photon energy shown by the arrow.

due to Raman scattering. However, this interpretation is ruled out by the fact that they disappear above a certain exciting energy, and even more significant, above a certain temperature. The temperature dependence from 2 to 16 K of the emission spectrum excited at 2.107 eV is shown in Fig. 6. While the broader features change little with temperature, the sharp lines broaden and disappear above  $T \sim 10$  K. As mentioned in Sec. II, this

broadening is probably due to two-phonon processes. Similar results are obtained for all excitation energies within the absorption tail. Raman scattering by LO phonons can be observed with laser excitation much below the emission band and its intensity does not depend on temperature up to 70 K. (The nonresonant Raman spectrum has been previously observed in  $\text{CdS}_x\text{Se}_{1-x}$  at temperatures up to 340 K.<sup>35</sup>)

It follows that the sharp lines are due to LO-assisted fluorescence from the narrow band of states excited by the laser. From the argument of Sec. II A we conclude that these states must be localized on the timescale of order 1 nsec, since they exhibit fluorescent line narrowing.

The sharp lines disappear quite abruptly over a range of less than 4 meV as the exciting energy is increased. This abruptness would be difficult to understand in terms of an increase in the phonon-assisted tunneling rate between localized states, since this rate is roughly proportional to  $g(\epsilon)$ , which increases by less than a factor of 2 over this energy range. The sharp disappearance at a certain energy seems to suggest, though it does not prove,

that exciton states are delocalized above this energy; i.e., that it is an effective mobility edge. As remarked earlier, this result, if true, is consistent with the generally accepted view that the exciton states at the band maximum are delocalized.

The accompanying sideband is unlikely to be an "ordinary" acoustic sideband; i.e., one involving phonon-assisted decay without exciton migration. Such a sideband is indeed observed at very low temperatures in GaP:N,<sup>36</sup> but in this case the no-phonon line is strongly forbidden, with a lifetime of microseconds, whereas in the present case the lifetime is less than 3 nsec, since the no-phonon transition is allowed. Bound excitons in CdS and CdSe do show a sideband,<sup>36,37</sup> but it is very much weaker relative to the nonphonon line than what we see here. Furthermore, as Fig. 5 shows, the sideband broadens as the excitation energy is increased: this would not be expected of an ordinary phonon sideband. Finally, Permogorov *et al.*<sup>13</sup> report induced polarization in the sideband; i.e., the emission retains some of the polarization of the exciting light, even when both polarizations are crystallographically equivalent. This polarization decreases monotonically with increasing separation from the sharp line. No such behavior is expected for a phonon sideband, which either retains the polarization of the no-phonon line (totally symmetric coupling) or loses it totally (phonon-induced transition).

We therefore attribute the sideband to emission from localized exciton states not resonant with the laser. Excitation is transferred to these states, with the emission of an acoustic phonon, within the exciton lifetime, as discussed in Sec. II C.

Complementary to the fluorescence data are the results of fluorescence excitation spectroscopy. In these experiments the fluorescence is monitored at a fixed wavelength (with a resolution better than 0.2 meV) while the exciting laser energy is continuously scanned, its intensity being kept constant. Figure 7 shows typical excitation spectra. The observed absorption spectrum is superimposed on the excitation in order to facilitate the interpretation. The two sharp lines at 25.5 and 37 meV again correspond to  $\text{LO}_1$  and  $\text{LO}_2$ , respectively. Above 8 K, the sharp lines disappear, as in the emission case.

As in the emission spectrum, the sharp lines are only seen in the  $x(yy)x$  geometry. Surprisingly, they are a factor of 2 sharper than in emission; we have checked that this is not instrumental effect, and we have no explanation for it. Because of this

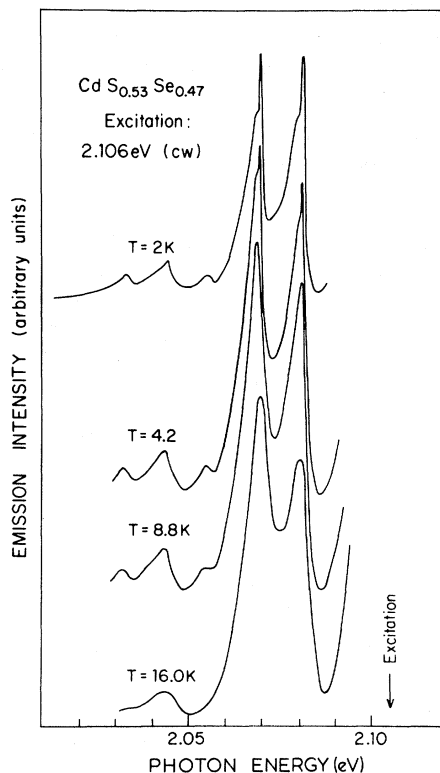


FIG. 6. Temperature dependence of the selectively excited emission spectrum:  $E_{\text{exc}} = 2.106$  eV.

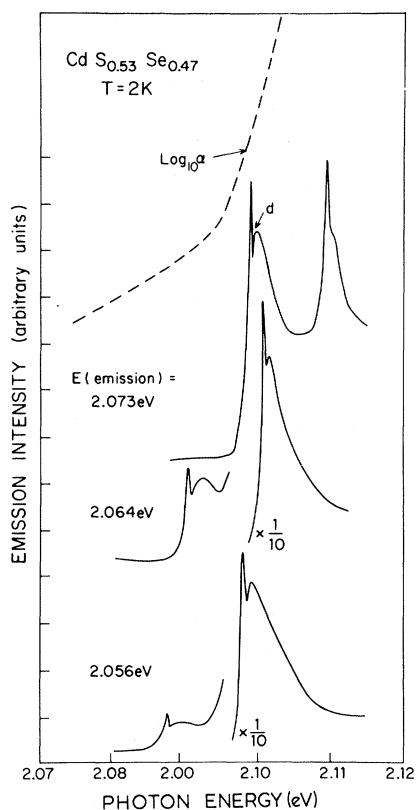


FIG. 7. Excitation spectrum of emission at the energies indicated under the same conditions as Fig. 5.

increased resolution a dip (marked *d* in Fig. 7) is visible on the high-energy side of the sharp line, showing that the sideband does indeed have a maximum as predicted theoretically. (In the fluorescence data the maximum is usually obscured by the tail of the sharp line.)

Fluorescence spectra at 2 K of samples with  $x=0.29$  and  $0.90$  are shown in Figs. 8 and 9. The data for  $x=0.29$  are similar to those for  $x=0.53$ , but for  $x=0.90$  the sidebands are always much broader than for smaller  $x$ . We will return to this point later.

#### A. Comparison of experimental results with theory

Typical fits to the theory of Sec. II of sidebands excited in the low-energy tail of the exciton band are shown in Figs. 10. In fitting, the ratio of the deformation-potential coupling parameter  $\delta_{DP}$  to the piezoelectric coupling parameter  $\delta_{PE}$  has been

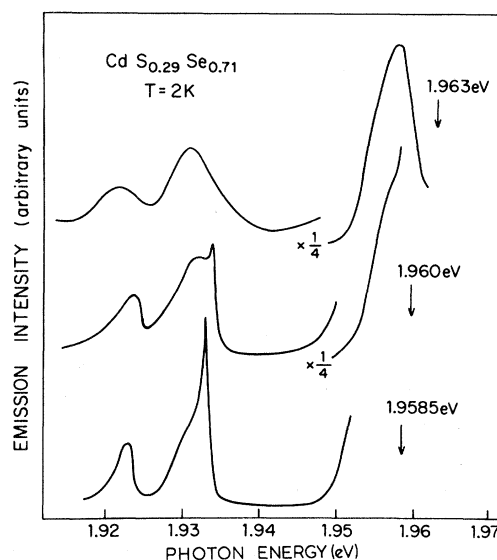


FIG. 8. Fluorescence excited by the indicated energies of  $\text{CdS}_x\text{Se}_{1-x}$ ,  $x=0.29$ .

treated as adjustable. For  $x=0.29$  [Fig. 10(a)] a good fit is obtained with piezoelectric coupling only, i.e.,  $G_D^2 \ll G_P^2$  as expected from the parameters of Table I. For  $x=0.53$  and  $x=0.90$  the deformation-potential contribution is more significant:  $\delta_{DP}/\delta_{PE}=0.06$  and  $0.8$ , respectively [Figs. 10(b) and 10(c)]. This is presumably a consequence of the effect of exciton localization on the effective deformation-potential coupling discussed in Sec.

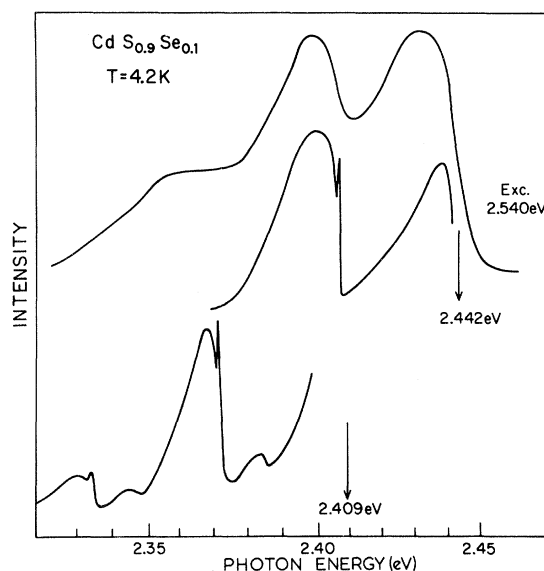


FIG. 9. Same as Fig. 8, with  $x=0.9$ .

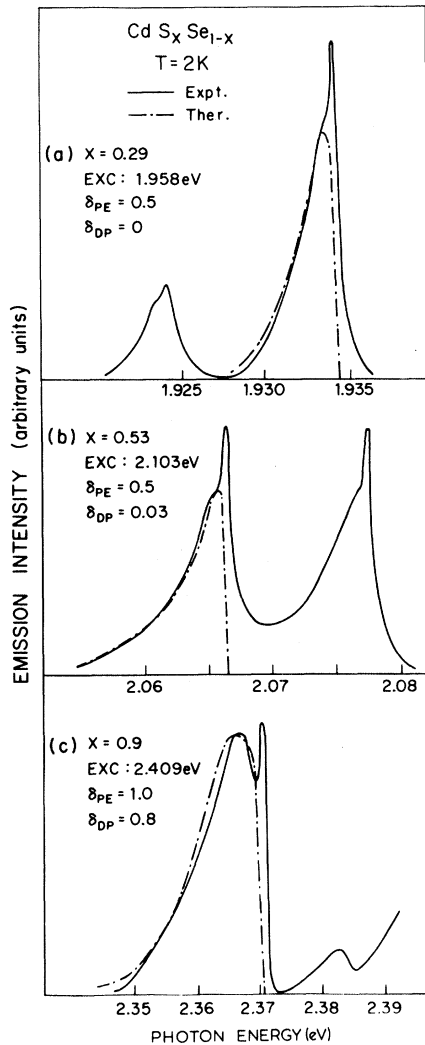


FIG. 10. Comparison of the theoretical sideband shape with experiment for (a)  $x=0.29$ , exciting energy  $E_{exc}=1.958$  eV; (b)  $x=0.53$ ,  $E_{exc}=2.103$  eV; (c)  $x=0.90$ ,  $E_{exc}=2.409$  eV;  $\delta_{PE}$ ,  $\delta_{DP}$  are the coupling coefficients for the piezoelectric interaction and deformation potential, respectively.

II C. As expected, the enhancement increases as  $a_B$  decreases. If this is the correct explanation, it is perhaps surprising that the fit is so good, since we might have expected a different  $q$  dependence for the deformation-potential coupling to excitons with different localization energy, in addition to the overall increase.

As the exciting energy is increased the fit deteriorates. The problem is apparent from Fig. 5(c); there is a broad nonresonant emission underlying the sharp lines and their sidebands. An esti-

mate of this emission is shown by the dashed line. When this background is subtracted, a reasonable fit to the sidebands can be obtained with a value of  $\delta$  increasing rapidly with energy, as expected. The broad background emission has a shape consistent with that obtained for laser energies so high that no sharp line emission is observed. If we attribute this emission to excitations of nonlocalized excitons, it follows that localized and delocalized states do overlap somewhat in energy, i.e., the effective mobility edge  $E_{em}$  is not sharply defined.

Another problem arises in the low-energy region. The theory of Sec. II predicts that the overall strength of the sideband relative to the sharp line (i.e., the product  $\tau\delta$ ) should drop off as  $g(E_a)$ ; this is not observed. We tentatively attribute this discrepancy to macroscopic broadening. At any excitation energy, the laser will predominantly excite those regions where  $E_x$  is lowest and  $g(E_a)$  is consequently highest; so these will always dominate the emission.

## V. CONCLUSIONS

We have shown that fluorescence line narrowing occurs under selective excitation of the low-energy side of the intrinsic exciton absorption line in  $\text{CdS}_x\text{Se}_{1-x}$  below about 10 K. We have argued that this is evidence for exciton localization, on a timescale of the order of nanoseconds, by alloy fluctuations. There is at present no satisfactory theory of such localization and of its spectral consequences, and our arguments are essentially qualitative. The abrupt disappearance of the narrowed line above a certain energy suggests the existence of an effective mobility edge.

A sideband to the sharp line emission is also observed. This can be qualitatively, and in a certain range of parameters quantitatively, accounted for by the theory of phonon-assisted tunneling between localized states presented in Sec. II. Further understanding of this remarkable model system requires dynamic measurements of fluorescence with subnanosecond resolution. Such experiments are in preparation.

## ACKNOWLEDGMENTS

We are grateful to M. V. Klein, S. Permogorov, and C. Weisbuch for helpful discussions, and for

communicating their unpublished work; to U. Levy, S. Chu, and J. Hegarty for helpful comments on the manuscript; to R. Beserman for providing the  $\text{CdS}_x\text{Se}_{1-x}$  crystals; and to R. C. Dunne and H. Katz for expert technical assistance. Part of

this work was done at the Physics Department and Solid State Institute, Technion, Haifa, Israel, where it was supported in part by The Israel Academy of Sciences and Humanities—Basic Research Foundation.

- \*Permanent address: Physics Department and Solid State Institute, Technion, Haifa, Israel.
- <sup>1</sup>T. Holstein, S. K. Lyo, and R. Orbach, in *Laser Spectroscopy*, edited by W. M. Yen (Springer, Berlin, 1981), p. 39.
  - <sup>2</sup>D. Huber, in *Laser Spectroscopy*, edited by W. M. Yen (Springer, Berlin, 1981), p. 39.
  - <sup>3</sup>J. Hegarty, D. L. Huber, and W. M. Yen, *Phys. Rev.* **23**, 6271 (1981).
  - <sup>4</sup>J. Klafter and J. Jortner, *J. Chem. Phys.* **68**, 1513 (1978).
  - <sup>5</sup>P. J. Wiesner, R. A. Steet, and H. D. Wolf, *Phys. Rev. Lett.* **35**, 1366 (1975).
  - <sup>6</sup>O. Goede, L. John, and D. Henning, *Phys. Status Solidi B* **89**, K183 (1978); O. Goede, D. Henning, and L. John, *ibid.* **B 96**, 671 (1979).
  - <sup>7</sup>L. G. Suslina, A. G. Plyukhin, D. L. Federov, and A. G. Areshkin, *Fiz. Tekh. Poluprovodn.* **12**, 2238 (1978) [*Sov. Phys.—Semicond.* **12**, 1331 (1978)].
  - <sup>8</sup>M. G. Craford and N. Holonyak, in *Optical Properties of Solids: New Developments*, edited by B. O. Seraphin (North-Holland, Amsterdam, 1976), p. 187.
  - <sup>9</sup>R. Dingle, R. A. Logan, and J. R. Arthur, in *GaAs and related compounds*, edited by C. Hilsum (Institute of Physics, Bristol, 1977), p. 210.
  - <sup>10</sup>N. F. Mott and E. A. Davis *Electronic Processes in Non-Crystalline Materials*, 2nd ed. (Oxford University Press, Oxford, England, 1979).
  - <sup>11</sup>R. Ulbrich and C. Weisbuch (unpublished).
  - <sup>12</sup>E. Cohen and M. D. Sturge, *Bull. Am. Phys. Soc.* **27**, 58 (1982).
  - <sup>13</sup>S. Permogorov, A. Reznitsky, V. Travnikov, S. Verbin, G. O. Mueller, and M. Nikofova, *Proceedings of International Conference on Luminescence, Berlin, 1981*, edited by I. Broser, H.-E. Gumlich, and R. Broser (North-Holland, Amsterdam, 1981), p. 409; S. Permogorov, A. Reznitsky, V. Travnikov, S. Verbin, G. O. Mueller, P. Floegel, and M. Nikofova; *Phys. Status Solidi B* **106**, K83 (1981).
  - <sup>14</sup>D. G. Thomas and J. J. Hopfield, *Phys. Rev.* **122**, 35 (1961); J. Voigt, F. Spiegelberg, and M. Senover, *Phys. Status Solidi* **91**, 189 (1979).
  - <sup>15</sup>R. G. Wheeler and J. O. Dimmock, *Phys. Rev.* **125**, 1805 (1977).
  - <sup>16</sup>S. D. Baranovski and A. L. Efros, *Fiz. Tekh. Poluprovodn.* **12**, 2233 (1978) [*Sov. Phys.—Semicond.* **12**, 1328 (1978)].
  - <sup>17</sup>B. Halperin and M. Lax, *Phys. Rev.* **148**, 722 (1966).
  - <sup>18</sup>S. Lai and M. V. Klein, *Phys. Rev. Lett.* **44**, 1087 (1980).
  - <sup>19</sup>V. Sayakanit, *Phys. Rev. B* **19**, 2266 (1979).
  - <sup>20</sup>P. D. Antoniou and E. N. Economou, *Phys. Rev. B* **16**, 3768 (1977).
  - <sup>21</sup>E. Yamaguchi, H. Aoki, and H. Kamimura, *J. Phys. C* **12**, 4801 (1979); S. D. Baranovski, B. Shlovskii, and A. I. Efros, *Zh. Eksp. Teor. Fiz.* **78**, 395 (1980); [*Sov. Phys.—JETP* **51**, 199 (198)].
  - <sup>22</sup>A. I. Anselm and Yu. A. Firsov, *Zh. Eksp. Teor. Fiz.* **28**, 151 (1955) [*Sov. Phys.—JETP* **1**, 139 (1955)].
  - <sup>23</sup>E. M. Conwell, *High field transport in semiconductors*, Solid State Physics Suppl. 9 (Academic, New York, 1962).
  - <sup>24</sup>G. D. Mahan in *Polarons in Ionic Crystals and Polar Semiconductors*, edited by J. T. De Vreese (North-Holland, Amsterdam, 1972), p. 553.
  - <sup>25</sup>A. R. Hutson, *J. Appl. Phys.* **32**, S 2287 (1961).
  - <sup>26</sup>A. I. Anselm and Y. A. Firsov, *Zh. Eksp. Teor. Fiz.* **30**, 719 (1956) [*Sov. Phys.—JETP* **3**, 564 (1956)].
  - <sup>27</sup>J. L. Merz, A. Baldereschi, and A. M. Sergent, *Phys. Rev. B* **6**, 3082 (1972); H. Mathieu, L. Bayo, J. Camassel, and P. Merle, *ibid.* **22**, 4834 (1980).
  - <sup>28</sup>M. V. Kein, private communication, 1981.
  - <sup>29</sup>P. M. Selzer, D. S. Hamilton, and W. M. Yen, *Phys. Rev. Lett.* **38**, 858 (1977).
  - <sup>30</sup>D. L. Huber and W. Y. Ching, *Phys. Rev. B* **18**, 5320 (1978).
  - <sup>31</sup>M. H. L. Pryce in *Phonons*, edited by R. W. H. Stevenson (Plenum, New York, 1966).
  - <sup>32</sup>C. H. Henry, K. Nassau, and J. W. Shiever, *Phys. Rev. B* **4**, 2453 (1971).
  - <sup>33</sup>M. P. Lisita, L. F. Gudymenko, V. N. Malinko, and S. F. Terekhova, *Phys. Status Solidi* **31**, 389 (1969).
  - <sup>34</sup>K. F. Rodgers (unpublished).
  - <sup>35</sup>M. Hayek and O. Brafman, in *Light Scattering in Solids*, edited by M. Balkanski (Flammarion, Paris, 1971), p. 26.
  - <sup>36</sup>P. J. Dean, *J. Lumin.* **1/2**, 398 (1970).
  - <sup>37</sup>J. J. Hopfield *Proceedings of the Eighth International Conference on the Physics of Semiconductors*, edited by A. C. Strickland (Bartholemew, Dorking, 1962), p. 75.